

# Numerical Simulation of the Kurtosis Effect on the EHL Problem

S. Gao, S. Srirattayawong

**Abstract**—In this study, a computational fluid dynamics (CFD) model has been developed for studying the effect of surface roughness profile on the EHL problem. The cylinders contact geometry, meshing and calculation of the conservation of mass and momentum equations are carried out using the commercial software packages ICEMCFD and ANSYS Fluent. The user defined functions (UDFs) for density, viscosity and elastic deformation of the cylinders as the functions of pressure and temperature are defined for the CFD model. Three different surface roughness profiles are created and incorporated into the CFD model. It is found that the developed CFD model can predict the characteristics of fluid flow and heat transfer in the EHL problem, including the main parameters such as pressure distribution, minimal film thickness, viscosity, and density changes. The results obtained show that the pressure profile at the center of the contact area directly relates to the roughness amplitude. A rough surface with kurtosis value of more than 3 has greater influence over the fluctuated shape of pressure distribution than in other cases.

**Keywords**—CFD, EHL, Kurtosis, Surface roughness.

## I. INTRODUCTION

LUBRICATION systems have attracted extensive research over the years as they are the lifeblood of all mechanical machines with moving parts. Essentially, effective lubrication techniques can help reduce frictional forces, as well as prevent and reduce the wear that can occur on all moving parts that come into contact with each other. Different methods have been developed, simple and complex, for solving such problems.

In 1886, Osborne Reynolds [1] presented the classical equation that is used to state the relationship between the motion and viscosity of the lubricant. The Reynolds equation has since been used widely to study laminar flows for the Newtonian fluids in hydrodynamics lubrication problems. Petrusevich [2] was the first person to solve the elastohydrodynamic lubrication (EHL) line contact problem and obtained the full numerical solution in 1951. Dowson and Higginson [3] suggested in 1959 a numerical method applicable to the EHL line contact problems, mainly suitable for highly loaded cases. Okamura [4] applied the Newton Raphson method to the solution of the Reynolds equation and managed to avoid the problem using iterative methods. Hamrock and Dowson [5] published their work in 1976 on how Gauss Seidel relaxation can be applied to the EHL point contact problem. This technique is successful when it is used

to solve the EHL line contact problem, but it still takes a long time to get a converged solution in the case of a point contact. In 1987, Lubrecht [6] suggested the use of a Multigrid technique, designed to significantly speed up the evaluation of the integrals.

The effects of surface roughness on hydrodynamic lubrication problems were usually studied by creating a model with a general roughness pattern, and most roughness models were included in the film thickness equation. In 1978, Patir and Cheng [7] studied the effect of surface roughness on the hydrodynamic lubrication problem by creating a model for a general roughness pattern. This model is useful for studying surface roughness effects, but real roughness is not isotropic. Then, in 1992, Venner and Napel [8] determined the roughness profile by measuring the actual surface of the material. They concluded that the surface texture significantly influences the pressure profile and the film thickness.

Commercial CFD software was employed in 2002 to simulate the EHL line contact problem by Almqvist et al. [9]. They compared the solutions of the EHL problem using both the Reynolds equation and the CFD method. They found that the results from both methods have good agreement in general. However, a small deviation is found in the case of thin film thicknesses. Then, in 2008, Hartinger et al. [10] carried out their CFD study of the thermo-elastohydrodynamic lubrication (TEHL) line contact problem. The free package OPENFOAM was used to solve the TEHL problem. The results between the Reynolds equation and the CFD model are similar and there is only a small difference between the predictions for high viscosity cases.

More recently, in 2012, the effects of surface roughness on the EHL problem using CFD techniques have been studied by the current authors [11]. The commercial software ICEM CFD and ANSYS Fluent have been used to create the geometry and solve the coupled fluid and structure equations. The resultant finding is that the surface roughness has significant influence on the fluid flow pattern and pressure distribution. The authors also studied the effects of the rough surface when applied loads and SRR ratios are varied. It is shown that the CFD model can be used effectively to predict the surface roughness effects on the EHL line contact problem. However, the CFD model was defined to be isothermal, whilst the thermal effects should be considered with respect to the lubricant properties such as density and viscosity.

Generally speaking, advances in CFD techniques have progressed significantly over the past decade, and commercial software capable of modeling fluid flows is now readily available. Also, improvement in computer processing power

S. Gao is with the Department of Engineering, University of Leicester, Leicester LE1 7RH, UK (corresponding author: phone: +44(0)116 252 2536; fax: +44(0)116 252 2525; e-mail: sg32@le.ac.uk).

S. Srirattayawong is with the School of Engineering, University of Phayao, 19 Moo 2, Maeka, Phayao 56000, Thailand (e-mail: Sutthinan.sr@up.ac.th).

means that data can be evaluated quickly. Using a CFD simulation approach has the advantage of allowing researchers to study and analyze the characteristics of fluid flow without creating real physical models. Therefore, the CFD approach has been chosen in this project to investigate the effects of real surface roughness on the TEHL problem.

## II. NOMENCLATURE

$E$	[Pa]	Reduced modulus of elasticity
$f$	[-]	Volume fraction
$h_o$	[m]	The minimum film thickness
$h_i$	[m]	Film thickness
$I$	[-]	Unit tensor
$L$	[Nm <sup>-1</sup> ]	Applied load per unit width
$p$	[Pa]	Pressure
$p_{sat}$	[Pa]	Liquid saturation vapour pressure
$R$	[m]	Reduced radii of curvature
$R(i)$	[m]	Surface roughness term
$SRR$	[-]	Slide to roll ratio = $2(u_p - R_c w_c) / (u_p + R_c w_c)$
$\Delta t$	[s]	Time step
$u$	[m/s]	Velocity
$V_{ch}$	[-]	A characteristic velocity
$x_i$	[m]	Cartesian axis in $i$ direction
$z$	[-]	Viscosity index

### Special character

$\rho$	[kg/m <sup>3</sup> ]	Density
$\tau$	[Pa]	Viscous stress tensor
$\eta$	[Pa·s]	Viscosity of Newtonian fluid
$\eta_o$	[Pa·s]	Viscosity at ambient pressure
$\xi$	[-]	Coordinate transformed range for numerical
$\sigma$	[kg·s <sup>-2</sup> ]	integration
$\phi$	[-]	Surface tension of the liquid
		The net rate of flow in a fluid element

### Subscripts

$a$	Average
$c$	Cylinder
$p$	Plate
$in$	At the inlet position
$out$	At the outlet position
$i$	At any node
$o$	Ambient or reference
$l$	Liquid phase
$v$	Vapour phase
$m$	Mixture phase
$sat$	Saturation vapour pressure

## III. GOVERNING EQUATIONS

The characteristics of fluid flow and heat transfer in the TEHL problem can be described by the fundamental conservation laws. This combines the continuity equation, momentum equation, and energy equation which are listed below:

### Continuity Equation:

$$\frac{\partial \rho}{\partial t} + \nabla \cdot (\rho \bar{u}) = 0 \quad (1)$$

### Momentum Equation:

$$\frac{\partial (\rho \bar{u})}{\partial t} + \nabla \cdot (\rho \bar{u} \bar{u}) = -\nabla p + \nabla \cdot \tau \quad (2)$$

where

$$\tau = -\eta (\nabla \bar{u} + (\nabla \bar{u})^T) + \frac{2}{3} \eta \bar{\nabla} \cdot \bar{u}$$

### Energy Equation:

$$\frac{\partial (\rho T)}{\partial t} + \nabla \cdot (\rho \mathbf{u} T) = \nabla \cdot (k \nabla T) + S_r \quad (3)$$

### A. Film Thickness Equation

The distribution of film thickness is dependent on the physical geometry of the cylinder and the elastic deformation of contact which is governed by the pressure distribution over the contact [12]. Generally, the surface texture is considered in the EHL line contact problem by including the surface roughness in the equation of film thickness. Therefore, the film thickness equation can be written as

$$h_i = h_o + \frac{x^2}{2R} + R(i) - \frac{2}{\pi E} \int_{-\infty}^{\infty} p(\xi) \ln(x - \xi)^2 d\xi \quad (4)$$

### B. Load Balance Equation

In order to simulate the EHL problem, the gap between the cylinder and the bottom plate has to be corrected in each iteration and updated until the generated pressure is equal to the applied load:

$$h_o^{new} = h_o^{old} + defect \quad (5)$$

where

$$defect = L - \int_{-\infty}^{\infty} p_i dx$$

### C. Density Equation

The density of fluid is affected when the pressure of lubricants changes. There is a linear variation between pressure and density, as Dawson and Higginson presented [13]. The relation between pressure and density can be written as:

$$\rho_i = \rho_o \left( 1 + \frac{0.59 \times 10^{-9} p_i}{1 + 1.7 \times 10^{-9} p_i} \right) \quad (6)$$

### D. Viscosity Equation

The viscosity of fluid depends on the pressure, as proposed by [14]. The Roelands model is approximately used to describe the behavior of Newtonian fluids as given below:

$$\eta_i = \eta_o \exp \left\{ \left[ \ln \eta_o + 9.61 \right] \left[ -1 + \left( 1 + 5.1 \times 10^{-9} p_i \right)^{-1} \right] \right\} \quad (7)$$

### E. Cavitation Model

The Reynolds equation cannot model the cavitation region. All negative pressures calculated at the outlet are set to zero. However, the negative pressure can be dealt with by using a cavitation model, in conjunction with the CFD model for the EHL problem. The full cavitation model [15] used in this research is:

$$\frac{\partial (\rho_m f)}{\partial t} + \nabla \cdot (\rho_m \bar{v}_v f) = \nabla \cdot (\gamma \nabla f) + A - B \quad (8)$$

where  $A$  and  $B$  are given by

$$A = 0.02 \frac{V_{ch}}{\sigma} \rho_l \rho_v \sqrt{\frac{2(p_{sat} - p)}{3\rho_l}} (1 - f) \quad (9)$$

$$B = 0.01 \frac{V_{ch}}{\sigma} \rho_l \rho_v \sqrt{\frac{2(p - p_{sat})}{3\rho_l}} (f) \quad (10)$$

The density of a lubricant for a liquid phase is a function of pressure as defined in equation (6). Thus the density of the vapour phase should be calculated from the fraction equation. Therefore the density of a mixture phase can be written as:

$$\rho = \alpha_v \rho_v + \alpha_g \rho_g + (1 - \alpha_v - \alpha_g) \rho_l \quad (11)$$

#### F. Surface Roughness Profiles

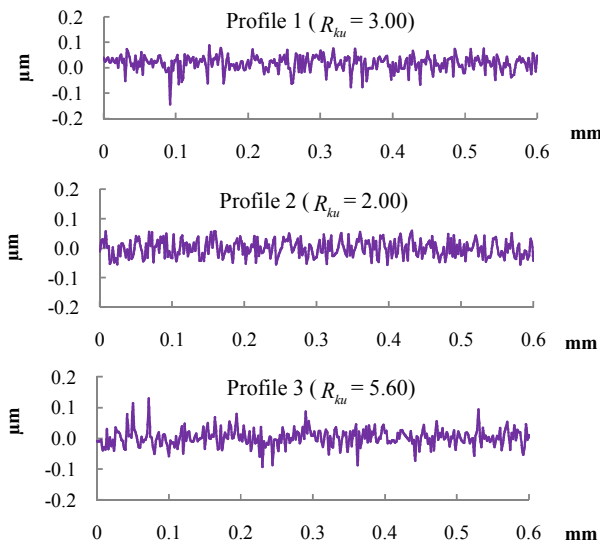


Fig. 1 Surface roughness profiles with different  $R_{ku}$

Three surface roughness profiles are generated using the MATLAB software. The Pearson distribution is employed to produce the random surface roughness. Fig. 1 shows the surface roughness profiles when the kurtosis parameter is varied, with  $R_{ku} = 3.0, 2.0$  and  $5.6$ , respectively. It can be observed that the values of high peaks and deep valleys of the surface roughness profile with  $R_{ku} = 5.60$  are higher than those of the other profiles.

#### IV. METHODOLOGY

The CFD model for two same-sized rollers, as presented in Fig. 2, is used to solve the EHL line contact problem in this study. The quadrilateral mesh generated by the CFD model is employed.

The quality of the spatial discretization of the CFD model must be verified to check whether the CFD mesh is sufficiently fine to calculate the pressure and velocity at the contact region within an acceptable engineering accuracy. The mesh resolution in the contact zone must be sufficiently fine to resolve this localised pressure change, whilst a coarse mesh

can be applied outside of the contact zone to reduce the simulation time. The minimum mesh size used in this CFD model is  $0.250 \mu\text{m}$  and the total number of cells is 23,474.

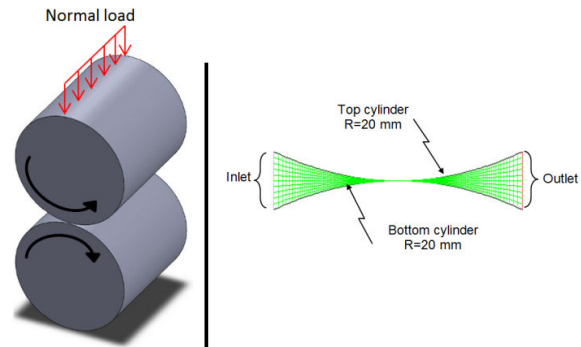


Fig. 2 Schematic view of the CFD model for the cylinders contact problem

TABLE I  
COMMON PARAMETERS

Parameters	Value	Unit
Input data		
- An applied load, $W$	50,000	N/m
- Average velocity, $U_a$	2.5	m/s
Solid properties (top and bottom cylinders)		
- Elastic modulus of solids, $E_1, E_2$	200	GPa
- Poisson's ratio of solids, $\nu_1, \nu_2$	0.30	-
- Specific heat of solids, $C_{p1}, C_{p2}$	460	J/Kg-K
- Density of solids, $\rho_1, \rho_2$	7850	kg/m <sup>3</sup>
- Thermal conductivity, $k_1, k_2$	47	W/m-K
Lubricant properties		
- Inlet viscosity of lubricant, $\eta_0$	0.01	Pa-s
- Vapour dynamic viscosity, $\mu_v$	$8.97 \times 10^{-6}$	Pa-s
- Liquid density, $\rho_l$	846.0	kg/m <sup>3</sup>
- Vapour density, $\rho_v$	0.0288	kg/m <sup>3</sup>
- Thermal conductivity of lubricant, $k$	0.15	W/m-K
- Temperature-viscosity coefficient of lubricant, $\gamma$	$6.4 \times 10^{-4}$	1/K
- Specific heat of lubricant, $C_p$	2,300	J/Kg-K
- Thermal expansivity of lubricant, $\beta$	$4.5 \times 10^{-4}$	1/K
- Pressure-viscosity coefficient, $z$	0.689	-

The boundary conditions and the initial condition used in this study are defined as follows:

- $P_{inlet} = 0 \text{ Pa}$
- $P_{outlet} = 0 \text{ Pa}$

The surface roughness profiles 1, 2, and 3 from Fig. 1 are applied to the surfaces of the top cylinder for the case study 1, 2, and 3, respectively. The solid and fluid properties used for the CFD simulations are listed in Table I.

#### V. SIMULATION RESULTS

The CFD model used in this study is validated by comparison with the result from the Reynolds equation. It is found that the pressure distribution and film thickness of the CFD model and the Reynolds equation are in good agreement. The maximum deviation of the peak pressure is 0.78%, and

the maximum deviation of the minimum film thickness is 1.73%.

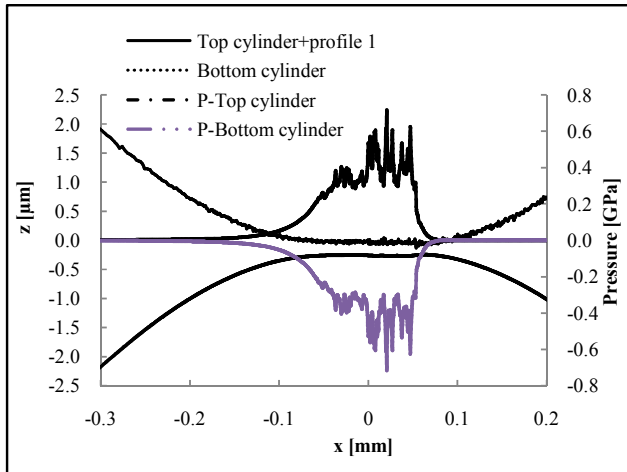


Fig. 3 Effect of surface roughness when the top cylinder is rough,  $R_{ku}=3.0$

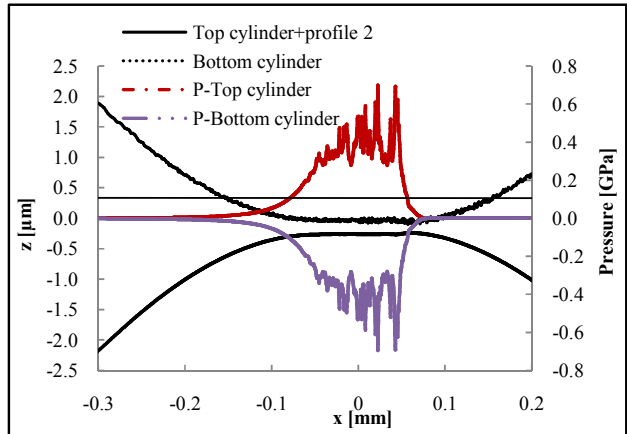


Fig. 4 Effect of surface roughness when the top cylinder is rough,  $R_{ku}=2.0$

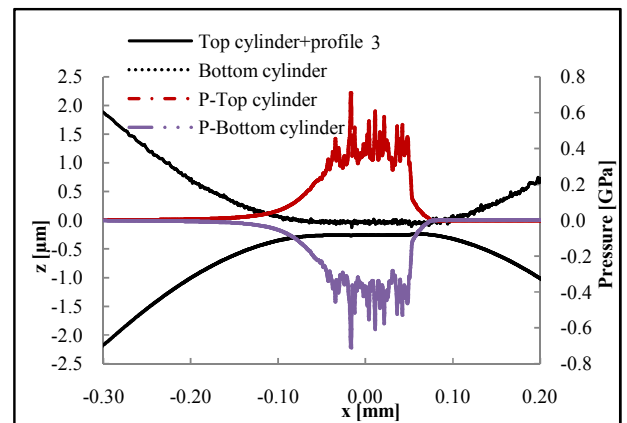


Fig. 5 Effect of surface roughness when the top cylinder is rough,  $R_{ku}=5.6$

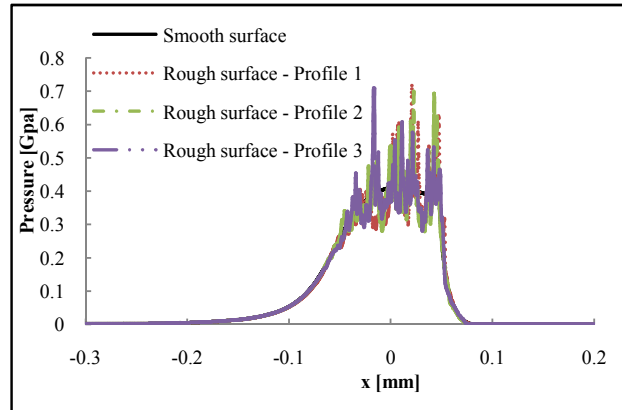


Fig. 6 Effect of surface roughness on pressure distributions with different kurtosis ( $R_{ku}$ ) values

Figs. 3-5 show the pressure distribution and the oil film thickness between the conjunction of the top and bottom cylinders with different  $R_{ku}$  values. It can be clearly seen that the surface roughness profile is significant to the behaviour of the fluid flow in the contact area. The generated pressures in the fluid film fluctuate when the surface roughness is applied. The kurtosis parameter evidently plays an important role in determining the pressure distribution and the cylinder surface deformation. Fig. 3 shows the pressure distribution and the oil film thickness for  $R_{ku} = 3$ , as a comparison with the other two cases. When the roughness profile with a kurtosis value less than 3 is applied, it is observed in Fig. 4 that the generated pressures fluctuate according to the roughness profile and that the average oil film thickness is closer to the case of smooth surface contact. For  $R_{ku} > 3$ , Fig. 5 reveals that the pressure fluctuation amplitude is higher than in the previous case, but the average oil film thickness is lower than the case where  $R_{ku} < 3$ . The direct comparison of the pressure distribution with three  $R_{ku}$  values is presented in Fig. 6. It can be seen that the highest pressure occurs in the  $R_{ku} > 3$  case as the fluid film is driven by the high peaks and deep valleys of the rough surface. Furthermore, it is found that the friction coefficient is inversely correlated to the kurtosis values. This may be due to the fact that the peaks of the rough profile can help reduce the area of contact. Other influencing parameters have also been investigated in this project, and the results will be reported elsewhere.

## VI. CONCLUSION

In this study, the effects of the surface roughness profile on the characteristic of the EHL problem are investigated using the developed CFD model. It is clearly shown that the surface roughness profile significantly influences the pressure distribution and the film thickness profile:

- If kurtosis  $R_{ku} < 3$ , the average oil film thickness is similar to that found in the smooth contact case.
- If  $R_{ku} > 3$ , the average oil film thickness and the friction coefficient are reduced.

- The friction coefficient is inversely correlated to the kurtosis value.

## ACKNOWLEDGMENT

The authors gratefully acknowledge the financial support from the Ministry of Science and Technology of Thailand for this project.

## REFERENCES

- [1] O. Reynolds, "On the theory of lubrication and its application to Mr. Beauchamp Tower's experiments, including an experimental determination of the viscosity of olive oil," *Philosophical Transactions of the Royal Society of London*, vol. 177, pp. 157-234, 1886.
- [2] A. I. Petrusevich, "Fundamental conclusions from the contact-hydrodynamic theory of lubrication," *Izv. Akad. Nauk. SSSR (OTN)*, vol. 2, pp. 209-223, 1951.
- [3] D. Dowson and G. R. Higginson, "A numerical solution to the elasto-hydrodynamic problem," *Journal of Mechanical Engineering Science*, vol. 1, pp. 6-15, 1959.
- [4] H. Okamura, "A contribution to the numerical analysis of isothermal elastohydrodynamic lubrication," *Proc. 9th Leeds-Lyon Symp. on Tribology*, pp. 313-320, 1983.
- [5] B. J. Hamrock and D. Dowson, "Isothermal elastohydrodynamic lubrication of point contacts, Part 1- Theoretical formulation. Journal of tribology," *Transactions of the ASME*, vol. 98, pp. 223-229, 1976.
- [6] A. A. Lubrecht, T. N. W.E., and R. Bosma, "Multigrid, an alternative method of solution for two-dimensional elastohydrodynamically lubricated point contact calculations," *Trans. ASME. Journal of Tribology*, vol. 109, pp. 437-443, 1987.
- [7] N. Patir and H. S. Cheng, "An Average Flow Model for Determining Effects of Three-Dimensional Roughness on Partial Hydrodynamic Lubrication," *ASME, Journal of Lubrication Technology*, vol. 100, pp. 12-17, 1978.
- [8] C. H. Venner and W. E. Ten Napel, "Surface Roughness Effects in an EHL Line Contact," *ASME, Journal of Tribology*, vol. 114, pp. 616-622, 1992.
- [9] T. Almqvist and R. Larsson, "The Navier-Stokes approach for thermal EHL line contact solutions," *Tribology International*, vol. 35, pp. 163-170, 2002.
- [10] M. Hartinger, M. L. Dumont, S. Ioannides, D. Gosman, and H. Spikes, "CFD modeling of a thermal and shear-thinning elastohydrodynamic line contact," *Journal of Tribology*, vol. 130, pp. 179-180, 2008.
- [11] S. Gao and S. Srirattayawong, "CFD Prediction of the Effects of Surface Roughness on Elastohydrodynamic Lubrication under Rolling/Sliding Conditions," *Applied Mechanics and Materials*, vol. 184, pp. 86-89, 2012.
- [12] K. L. Johnson and J. L. Tevaarwerk, "The shear behaviour of elastohydrodynamic oil films," *Proc. R. Soc. London*, vol. 356, pp. 215-236, 1977.
- [13] R. Gohar, *Elastohydrodynamics*, England: Ellis horwood limited, 1988.
- [14] D. Dowson, G. Higginson, and A. Whitaker, "Elasto-hydrodynamic lubrication: a survey of isothermal solutions," *Journal of Mechanical Engineering Science*, vol. 4, pp. 121-126, 1962.
- [15] A.K. Singhal, M.M. Athavale, L. Huiying, L. Jiang, "Mathematical bases and validation of the full cavitation model," *Journal Fluids Engineering*, vol. 124, pp. 617-624, 2002.